

# Obtaining of Nanocrystalline Ferrites and Other Complex Oxides by Sol–Gel Method with Participation of Auto–Combustion

V. S. Bushkova

**Abstract**—It is well known that in recent years magnetic materials have received increased attention due to their properties. For this reason a significant number of patents that were published during the last decade are oriented towards synthesis and study of such materials. The aim of this work is to create and study ferrite nanocrystalline materials with spinel structure, using sol-gel technology with participation of auto-combustion. This method is perspective in that it is a cheap and low-temperature technique that allows for the fine control on the product's chemical composition.

**Keywords**—Magnetic materials, ferrites, sol-gel technology, nanocrystalline powders.

## I. INTRODUCTION

NOWADAYS ferrites are very topical objects and promising materials for the various practical applications [1]–[4]. The ferrite materials are widely used in the modern radioelectronics, the basic tendency of which is microminiaturization of the products. It should be noted that the ferrite memory is indispensable in cosmos and military industries in the conditions of hard electromagnetic radiation.

Complex oxide systems based on nickel, magnesium, iron, cobalt have been investigated intensely in order to obtain new materials for the ceramics production. Among these oxides phases with spinel structure are the most promising. Magnesium-zinc and nickel-aluminum ferrites are different from many other materials because they have important electrical, magnetic and mechanical properties. These ferrites are promising in SHF-technology, and they are used as a magnetic component in composite magnetoelectric materials [5]–[8].

During last decade several patents were published in the field of materials science in order to obtain and study complex oxide materials. Methods of deposition or mixing the components solid powders with the following stages of thermal treatment are the most common ways of such materials obtaining. It is rather difficult to obtain single-phase products by these methods.

In recent years in SHF-technology new trend in material science has appeared – the synthesis of various substances with nanometer-sized particles. This problem is a result of the nanocrystalline materials using, which have unique properties comparing with the macrocrystalline materials of the same

chemical composition. During the synthesis of ferromagnetic oxide nanomaterials special attention is paid to chemical methods of ferrite components homogenization [9]–[11]. This provides the high chemical homogeneity and activity of ferrite powders. Today sol-gel technology is an important and progressive method of nanomaterials with improved properties obtaining.

Developing the ideas of nanotechnology, we have patented a method of synthesis the ferrites with different chemical compositions for magnetic devices and components of electronic equipment – the sol-gel with participation of auto-combustion (SGA) [12]. In comparison with the ceramic method, SGA-technology is more simple and economical way of obtaining the nanocrystalline materials with high homogeneity, which increases their electromagnetic and mechanical properties.

## II. EXPERIMENTAL

In this paper ferrite systems  $Mg_{1-x}Zn_xFe_2O_4$  ( $x = 0, 0.2, 0.44, 0.5, 0.6$ ) and  $NiAl_xFe_{2-x}O_4$  ( $x = 0, 0.1, 0.2, 0.3, 0.4, 0.5$ ) were synthesized by SGA-technology. The main idea of this method is using heat of an exothermic reaction at the ferrites synthesis. In some cases this process (the use of exothermic reaction heat to maintain this reaction itself) is dynamic, that is the narrow high-temperature combustion zone is moving according to the model.

The synthesis of complex oxide materials by SGA-method involves the following stages: preparation of metal nitrates aqueous solutions in accordance with their stoichiometric ratio, adding of the optimum amount of citric acid, changing of the pH to 7 by adding of 25%  $NH_4OH$  solution, evaporation of the solution to the gel formation, drying of gel at low temperatures to the xerogel forming, controlled auto-combustion of xerogel with nanopowders forming. Magnesium and zinc oxides, metal nitrates with the chemical formula  $Me_n(NO_3)_m \times rH_2O$ ,  $Me = Ni, Al, Fe$ , nitric and citric acids were used as precursors.

The phase identification of powders was performed using X-ray diffraction (XRD). XRD patterns were recorded at room temperature with a DRON-3 diffractometer using  $Cu K\alpha$  radiation with  $\lambda = 1,5419 \text{ \AA}$  in air. Diffraction patterns were recorded in the scan range  $15^\circ$ – $65^\circ$  with a scan steep size of  $0.02^\circ$ . Surface morphology of the samples was investigated by a JEOL NeoScope JSM-5000 scanning electron microscope (SEM).

Thermal analysis of samples was conducted using

V. S. Bushkova is with the Vasyl Stefanyk Pre-Carpathian National University, Ivano-Frankivsk, 76025 Ukraine (phone: 034-222-2140; fax: 034-223-1574; e-mail: bushkovavira@rambler.ru).

simultaneous thermal analyzer STA 449 F3 Jupiter in the mode of the linear heating with rate of 10°C/min in the temperature range 25–1000°C; as a result curves of thermogravimetric (TG) and differential thermal analysis (DTA) were experimentally obtained. Change of mass at heating was determined with an accuracy of 10<sup>-6</sup> kg.

Infrared (IR) spectra for the gel precursor and the as-burnt powder were recorded on a NICOLETIS 10 spectrophotometer in the range 400–4000 cm<sup>-1</sup> by the KBr pellet method. Processing of the results was carried out in software OMNIC 8.1.

### III. RESULTS AND DISCUSSION

The SGA-method allows obtaining single-phase complex oxide materials with a high degree of dispersion. The technology of this method is to obtain materials with predetermined physical and chemical properties. This technology involves sol obtaining and consistent turning it into a gel. For example, for the synthesis of NiFe<sub>2</sub>O<sub>4</sub> ferrite material 1 mole of Ni(NO<sub>3</sub>)<sub>2</sub>·6H<sub>2</sub>O, 2 mol of Fe(NO<sub>3</sub>)<sub>3</sub>·9H<sub>2</sub>O, and 3 mol of C<sub>6</sub>H<sub>8</sub>O<sub>7</sub>·H<sub>2</sub>O (citric acid) were used. Presence of citric acid is explained as follows: it is believed that the formation of nitrate-citrate complexes of metals eliminates the differences in individual behavior of cations in solution. This enhances the mixing and allows to avoid separation of the components in the following stages of synthesis. Distilled water is used as the dispersion phase. At mixing the precursors hydrolysis and polycondensation reactions are taking place, which lead to the formation of a colloidal solution – sol – hydroxide particles whose size does not exceed a few nm.

Neutralization of the dispersion medium by means of 25% ammonia solution to the level of pH 7 results in the intensive formation of contacts between particles. This leads to the formation of monolithic gel in which the molecules of the solvent (water) are enclosed in a flexible, but rather strong three-dimensional network, which is formed by particles of hydroxides. The particles of the dispersed phase are connected in points of contact by forces of intermolecular interactions. In this case granting of energy to reaction system is necessarily to maintain the gel formation. By the way added energy is required for the following drying out the gel with the aim of converting it to the xerogel due to evaporation of dispersion medium. With subsequent drying, the dry gel begins to burn arbitrarily with the formation of ferrite powders with a spinel structure and the product of combustion.

In order to explain the process of nitrate-citrate xerogel auto-combustion, differential thermal and thermogravimetric analysis of the dried gel were carried out. Experimental observation showed that the dried gel, formed from metal nitrates and citric acid, was burned in the process auto-combustion, forming a fine powder. Fig. 1 shows the DTA and TG plots of the dried nitrate-citrate MgFe<sub>2</sub>O<sub>4</sub> gel. As it was expected, the decomposition reaction was strongly exothermic. At about 210°C the exothermic peak was observed. The weight change associated with this exothermic reaction was about 75%.

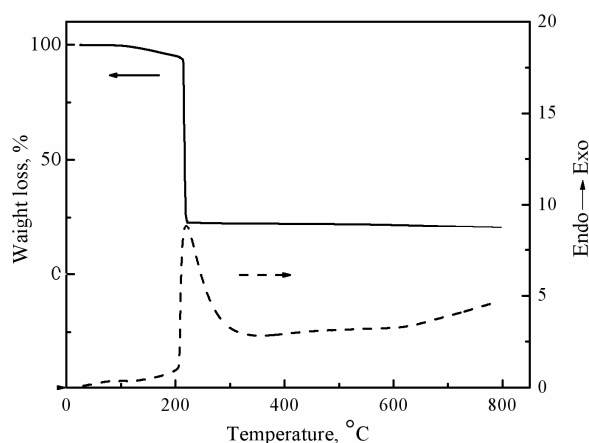


Fig. 1 DTA-TG curves of the nitrate-citrate xerogel

The auto-combustion process is as follows: ammonium nitrate decomposes at temperature of 210°C with evolution of oxygen. It is well known that oxygen accelerates the combustion process and great amount of heat generates in this exothermic reaction, that results in violent combustion. Also the effect of ferrite formation from the metal oxides promotes of the burning process. Since process can be finished in very short time, the particle size of the synthesized ferrite powders can remain small.

Fig. 2 shows the XRD patterns for the powder of studied NiAl<sub>x</sub>Fe<sub>2-x</sub>O<sub>4</sub> system. All the powders have phase of ferrite with spinel structure, similar to that of the as-sintered ceramic sample. This indicates that the Ni–Al ferrites can be directly formed after the auto-combustion of the gel.

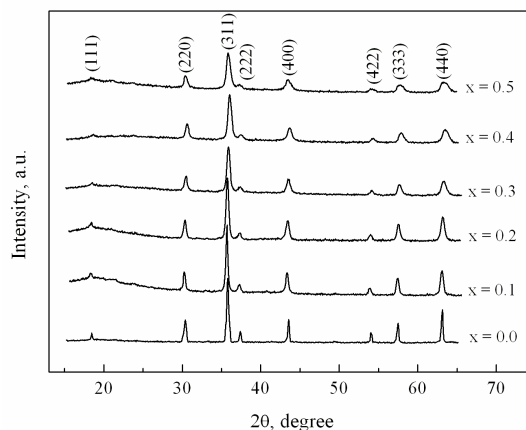


Fig. 2 XRD patterns of NiAl<sub>x</sub>Fe<sub>2-x</sub>O<sub>4</sub> samples

The average particles size of powders was calculated from the (311) diffraction peak using the Debye Scherrer formula:

$$\langle D \rangle = \frac{0.9\lambda}{\beta \cdot \cos\theta}, \quad (1)$$

where  $\lambda$  is the X-ray wavelength,  $\beta$  – the full width at half maximum,  $\theta$  – the Bragg angle.

The results shown in Fig. 3 depict that the increasing content of  $\text{Al}^{3+}$  ions decreases the particle size of Ni–Al ferrites. Though all the samples were prepared under identical condition, the particle size was not the same for all contents of  $\text{Al}^{3+}$ . This was probably due to the reaction condition, which favored the formation of new nuclei preventing further growth of particles when the  $\text{Al}^{3+}$  content was increased.

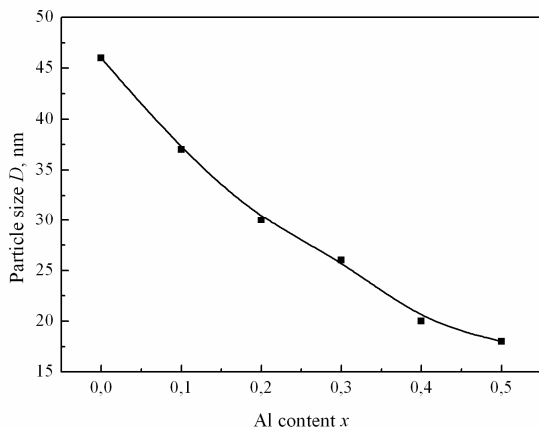


Fig. 3 Variation of particle size with Al content  $x$

X-ray diffraction patterns of the studied samples are shown in Fig. 4. The patterns confirm also the formation of single phase cubic spinel structure. The replacement of  $\text{Mg}^{2+}$  ions by  $\text{Zn}^{2+}$  ions leads to the presence of phase ZnO, the amount of which increases with parameter  $x$  in the system  $\text{Mg}_{1-x}\text{Zn}_x\text{Fe}_2\text{O}_4$ . The maximum content of phase ZnO is 3% of the total composition for sample  $\text{Mg}_{0.4}\text{Zn}_{0.6}\text{Fe}_2\text{O}_4$ . According to the X-ray diffraction, size of Mg–Zn ferrites particles are in the range of 20–35 nm.

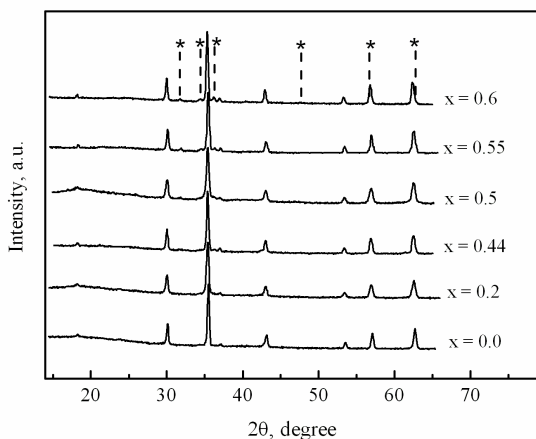


Fig. 4 XRD patterns of  $\text{Mg}_{1-x}\text{Zn}_x\text{Fe}_2\text{O}_4$  samples, \* – phase ZnO

Fig. 5 shows the morphology of the  $\text{Mg}_{0.5}\text{Zn}_{0.5}\text{Fe}_2\text{O}_4$  powder. The microphotograph gives an idea of the surface morphology of obtained ferrites. The morphology of the powder surface shows that obtained powder presents a regular

repartition of nearly-spherical grains in a flat pattern and a rather highly porous homogeneous surface. During the combustion process, a large amount of gaseous material is released that leading to forming of numerous microscopic pores in as-burnt powders. The micrograph shows the formation of powder consisting of highly agglomerated particles with an average particle size of not greater than 50 nm.

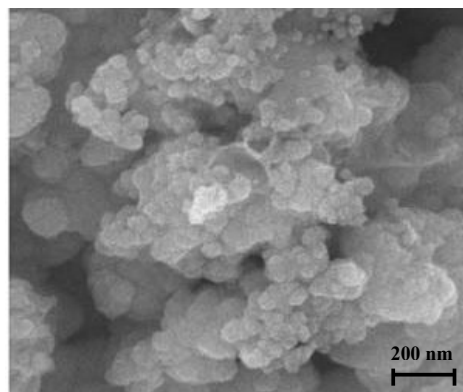


Fig. 5 SEM picture of  $\text{Mg}_{0.5}\text{Zn}_{0.5}\text{Fe}_2\text{O}_4$  powder

According to the obtained results of X-ray analysis and scanning electron microscopy it was determined that the synthesized powder was agglomerated, that is composed of several nanoparticles.

The lattice parameter ( $a$ ) was obtained by extrapolation of  $a$  for different indexed planes against the Nelson-Riley function. Since each primitive unit cell of the spinel structure contains eight molecules, the X-ray density ( $d_x$ ) was calculated by:

$$d_x = \frac{8M}{N_a a^3}, \quad (2)$$

where  $M$  is molecular weight of the particular ferrite,  $N_a$  is the Avogadro's number and  $a^3$  is the volume of the cubic unit cell.

The values of lattice parameters and X-ray density were obtained for all the samples using XRD data and are listed in Table I. It is observed that for  $\text{NiAl}_x\text{Fe}_{2-x}\text{O}_4$  systems the lattice parameter and X-ray density decreases with increasing  $\text{Al}^{3+}$  content  $x$ . This behavior of lattice parameter with aluminum content is explained on the basis of difference in ionic radii of  $\text{Al}^{3+}$  (0.51 Å) and  $\text{Fe}^{3+}$  (0.67 Å). In the present series, larger  $\text{Fe}^{3+}$  ions are replaced by smaller  $\text{Al}^{3+}$  ions; therefore, decrease in lattice constant takes places. Similar trend was found in Cu–Cd ferrite with aluminum substitution [13]. In the case of our samples, the lattice parameters were found to be slightly higher than those reported by others [14]. The decrease in  $d_x$  may be due to the fact that molecular weight of  $\text{NiAl}_x\text{Fe}_{2-x}\text{O}_4$  ferrites is lower than  $\text{NiFe}_2\text{O}_4$  ferrite.

The XRD parameters of  $\text{Mg}_{1-x}\text{Zn}_x\text{Fe}_2\text{O}_4$  systems show that  $a$  increases smoothly with the increase of  $\text{Zn}^{2+}$  content. The increase in lattice parameters is attributed to the larger ionic radius of  $\text{Zn}^{2+}$  (0.82 Å), which when substituted in the lattice

resides on the tetrahedral sites and displaces the smaller  $\text{Fe}^{3+}$  ( $0.67 \text{ \AA}$ ) ion from the tetrahedral sites to the octahedral sites at the expense of the  $\text{Mg}^{2+}$  ions ( $0.66 \text{ \AA}$ ). The results are in close agreement with the earlier values reported in the literature [15].

TABLE I  
STRUCTURAL PARAMETERS OF SYNTHESISED FERRITES

$\text{NiAl}_x\text{Fe}_{2-x}\text{O}_4$			$\text{Mg}_{1-x}\text{Zn}_x\text{Fe}_2\text{O}_4$		
$x$	$a$ ( $\text{\AA}$ )	$d_x$ ( $\text{kg/m}^3$ )	$x$	$a$ ( $\text{\AA}$ )	$d_x$ ( $\text{kg/m}^3$ )
0.0	8.3427	5.36	0.0	8.3834	4.51
0.1	8.3350	5.31	0.2	8.3897	4.69
0.2	8.3233	5.27	0.44	8.3962	4.88
0.3	8.3158	5.21	0.5	8.4025	4.93
0.4	8.2988	5.18	0.55	8.4067	4.98
0.5	8.2711	5.16	0.6	8.4067	5.01

Chemical and structural changes that take place during combustion can be monitored by a spectroscopic analysis. IR was performed on the obtained powders to understand the mechanism behind the auto-combustion reaction. Fig. 6 shows the IR spectra of the dried gel and the as-burnt powder in the range  $400\text{--}4000 \text{ cm}^{-1}$ .

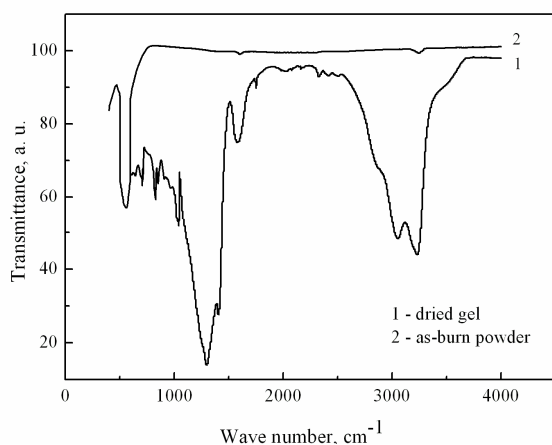


Fig. 6 IR spectra of the dried gel and as-burnt powder

The dried gel shows the characteristic bands at about  $1300$ ,  $1600$  and  $3250 \text{ cm}^{-1}$  corresponding to  $\text{NO}_3^-$  ion, carboxyl –  $\text{COO}^-$  group and the O-H group, respectively. The existence of the characteristic bands of  $\text{NO}_3^-$  indicated that the  $\text{NO}_3^-$  as a group exists in the structure of citrate gel during the gelation of the mixed solution formed from nitrates and citric acid. The band at about  $3050 \text{ cm}^{-1}$  is assigned to the stretching vibrations of the O-H groups of hydrogen bonding at short distances.

The spectrum of the as-burnt powder gives a significant band at  $560 \text{ cm}^{-1}$ , which is the characteristic band of  $\text{NiAl}_{0.5}\text{Fe}_{1.5}\text{O}_4$  ferrite. The absence of spectroscopic band corresponding to the carboxyl group and nitrate ion at  $1600$  and  $1300 \text{ cm}^{-1}$ , respectively, suggests that these groups take part in the reaction during the combustion process. Therefore, the combustion can be considered as a thermally induced anionic redox reaction of the gel wherein the citrate ion acts as

a reductant and the nitrate ion acts as an oxidant. This auto-combustion reaction forms the spinel structure of the ferrite with the evolution of heat.

#### IV. CONCLUSION

When using SGA-technology, despite the duration of the synthesis process, the consumption of initiating the reaction is much smaller than the energy needed for long time high-temperature annealing at ceramic synthesis. Thus, the SGA-method is an effective way of obtaining the ferrite samples with a given form due to gels polycondensation and their following compaction in which the transition sol – gel – ferrite powder during heat treatment occurs.

#### REFERENCES

- [1] A. V. Kopayev, V. S. Bushkova, "Application of the electron theory of sintering to the ferrite system," *Acta physica polonica A*, vol. 117, no. 1, pp. 25–28, 2010.
- [2] S. Krupichka, *Physics of ferrites and related magnetic oxides*. Moscow: World, 1976, 504 p.
- [3] A. V. Kopayev, B. K. Ostafiychuk, I. P. Yaremiy, I. Y. Vylka, "Structure and magnetic properties of Ni-Al-ferrite powders, synthesized by sol-gel method of auto-combustion," *Surface. X-ray, synchrotron and neutron study*, vol. 10, pp. 79–83, 2007.
- [4] A. V. Kopayev, B. K. Ostafiychuk, I. Y. Vylka, D. L. Zadnipyryanny, "Peculiarities of nickel-aluminium ferrites nanopowder structure," *Mat-wiss. u. Werkstofftech.*, vol. 40, no. 4, pp. 255–257, 2009.
- [5] A. V. Kopayev, V. S. Bushkova, J. M. Tafiychuk, D. L. Zadnipyryanny, "Electro-magnetic properties and imperfectness of composite of  $x\text{NiAl}_{0.5}\text{Fe}_{1.5}\text{O}_4-(1-x)\text{BaTiO}_3$ ," in *Proc. 11th Europhysical Conference on Defects in Insulating Materials PECS*, Hungary, 2010, p. A53.
- [6] V. S. Bushkova, A. V. Kopayev, "Study of electrical properties of composites  $(1-x)\text{NiAl}_{0.5}\text{Fe}_{1.5}\text{O}_4-x\text{BaTiO}_3$ ," *Eastern-European Journal of Enterprise Technologies*, vol. 10, no. 4/5, pp. 43–47, 2011.
- [7] S. C. Chae, P. Murugavel, J. H. Lee, H. J. Ryu, T. W. Noh, "Growth and Characterization of Epitaxial Barium Titanate and Cobalt Ferrite Composite Film," *Journal of the Korean Physical Society*, vol. 47, pp. 345–347, 2005.
- [8] R. P. Mahajan, K. K. Patankar, M. B. Kothale, S. C. Chaudhari, V. L. Mathe, S. A. Patil Mahajan, "Magnetolectric effect in cobalt ferrite–barium titanate composites and their electrical properties," *Pramana*, vol. 58, pp. 1115–1124, 2002.
- [9] A. G. Belous, E. V. Pashkov, V. A. Elshansky, V. P. Ivanitsky, "Influence of deposition conditions of iron hydroxides (III, II) on the phase composition, particle morphology and properties of the sediments," *Inorganic Materials*, vol. 4, pp. 431–439, 2000.
- [10] K.S. Martirosyan, P.B. Avakian, M.D. Nerseyan, "Phase formation in the process of self-propagating high temperature synthesis of ferrites," *Inorganic Materials*, vol. 4, pp. 489–492, 2002.
- [11] V.V. Popov, A.I. Gorbunov, "The hydrothermal crystallization of iron hydroxide (III)," *Inorganic Materials*, vol. 3, pp. 319–326, 2006.
- [12] A. Kopaev, V. Bushkova, B. Ostafiychuk, "Sol-Gel Synthese und Eigenschaften der weichmagnetischen Nanoferrite und Verbundwerkstoffen. Physik und Technologie der Nanoferrite mit dem Bariumtitanat," (monographie). Saarbrücken: Lap Lambert Academic Publishing, 2013, 154 p.
- [13] S.S. Suryawanshi, V.V. Deshpande, U.B. Deshmukh, S.M. Kabur, N.D. Chaudhari, S.R. Sawant, "XRD analysis and bulk magnetic properties of  $\text{Al}^{3+}$  substituted Cu–Cd ferrites," *Mat. Chem. Phys.*, vol. 59, no. 3, pp. 199–203, 1999.
- [14] A.T. Raghavender, R.G. Kulkarni, K.M. Jadhav, "Magnetic properties of nanocrystalline Al doped nickel ferrite synthesized by the sol-gel method," *Chinese Journal of Physics*, vol. 46, no. 3, pp. 366–375, 2008.
- [15] P.P. Hankare, V.T. Vader, U.B. Sankpal, L.V. Gavali, R. Sasikala, I.S. Mulla, "Effect of sintering temperature and thermoelectric power studies of the system  $\text{MgFe}_{2-x}\text{Cr}_x\text{O}_4$ ," *Solid State Sci.*, vol. 11, no. 12, pp. 2075–2079, 2009.